Electronic Supplementary Material (ESI) for Energy & Environmental Science.

Electronic Supplementary Information

Seamlessly Conductive $Co(OH)_2$ Tailored Atomically Dispersed Pt Electrocatalyst in Hierarchical Nanostructure for Efficient Hydrogen Evolution Reaction

Kai Ling Zhou,[a] Changhao Wang,*[a] Zelin Wang,[b] Chang Bao Han,*[a] Qianqian Zhang,[a] Xiaoxing Ke,[b] Jingbing Liu [a] and Hao Wang[a]

[a] College of Materials Science and Engineering, Beijing University of Technology, Beijing 100124, P. R. China
E-mail: cbhan@bjut.edu.cn; wangch33@bjut.edu.cn
[b] Institute of Microstructure and Properties of Advanced Materials, Beijing University of Technology, Beijing 100124, P. R. China.

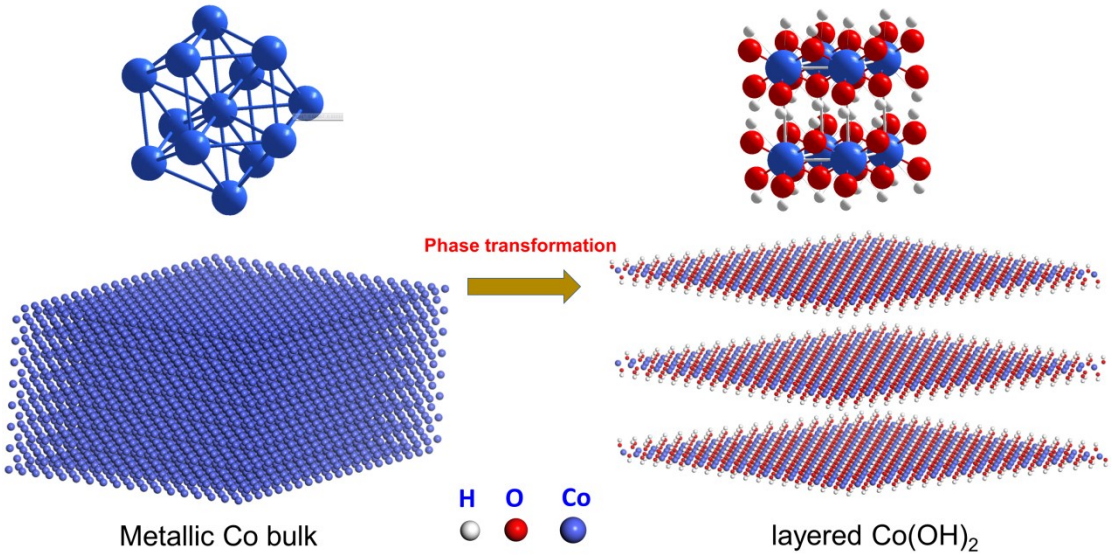

Figure S1. Schematic of the electrochemical phase transformation of metallic Co to layered $Co(OH)_2$.

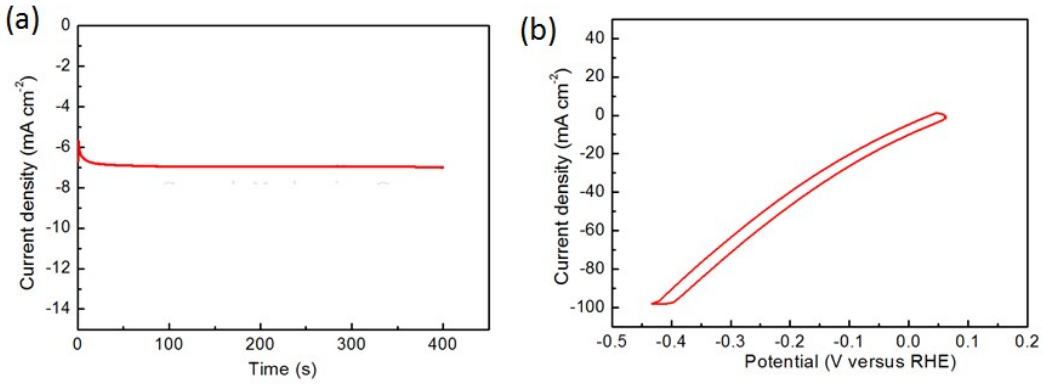

Figure S2. (a) The electrochemical deposition curve of metallic Co on Ag NWs templates and (b) one CV curve chosen from 3000 CV cycles for single-atom Pt immobilization and phase transformation of metallic Co to $Co(OH)_2$ on Ag NWs.

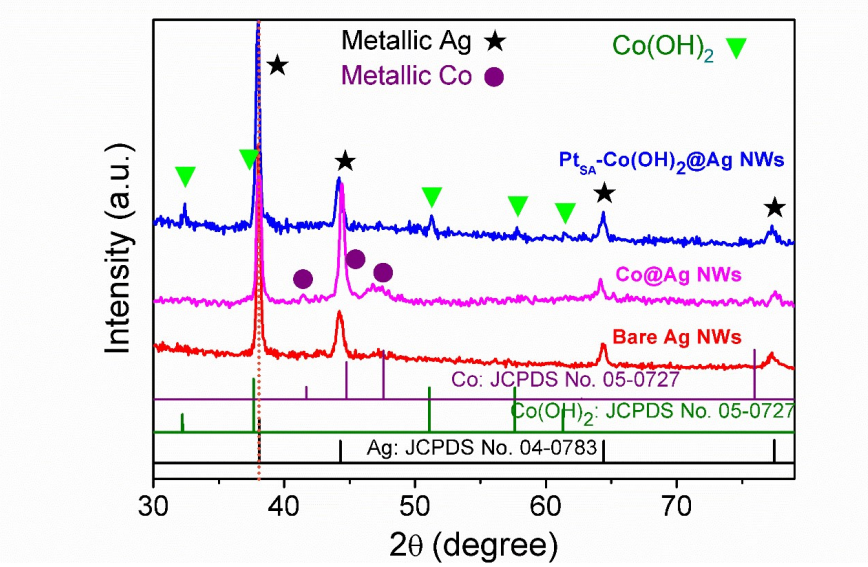

Figure S3. The X-ray diffraction (XRD) patterns of Pt_{SA}-$Co(OH)_2$@Ag NWs, Co @Ag NWs and Ag NWs.

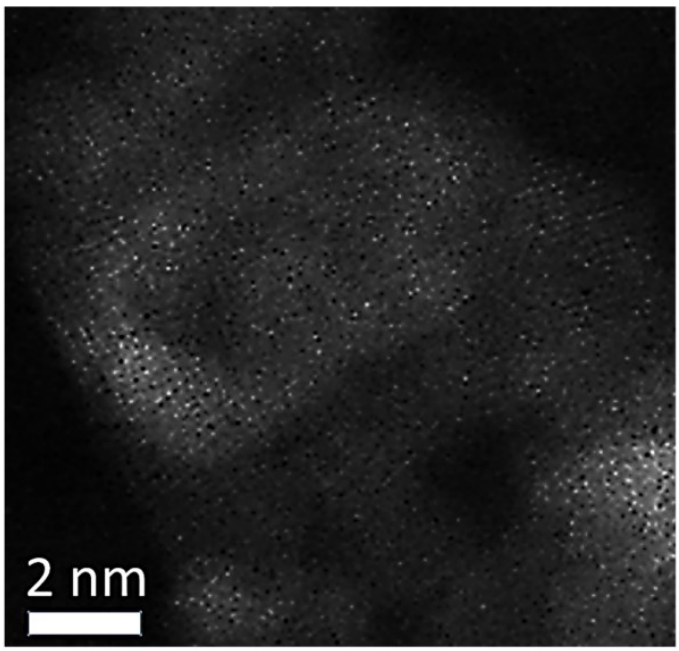

Figure S4. The aberration-corrected high-angle annular dark-field scanning TEM (HAADF-STEM) images of Pt_{SA}-$Co(OH)_2$ nanosheets.

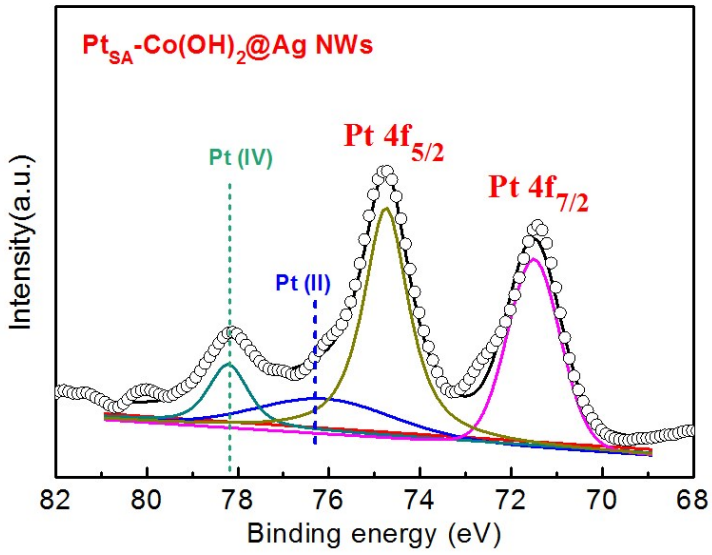

Figure S5. The Pt XPS fitting curve of Pt_{SA}-$Co(OH)_2$@Ag NWs.

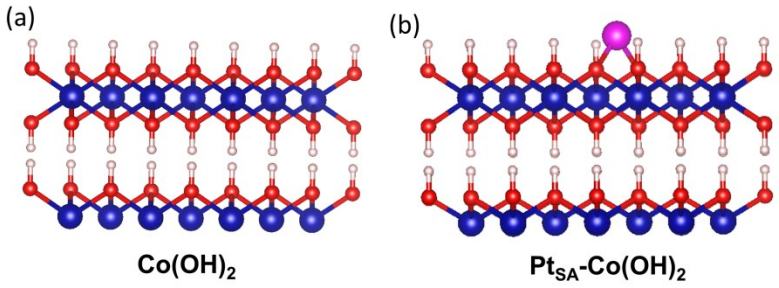

Figure S6. Computational models of (a) $Co(OH)_2$ and (b) Pt_{SA}-$Co(OH)_2$. H, white ball; Co, blue ball; O, red ball; Pt, pink ball.

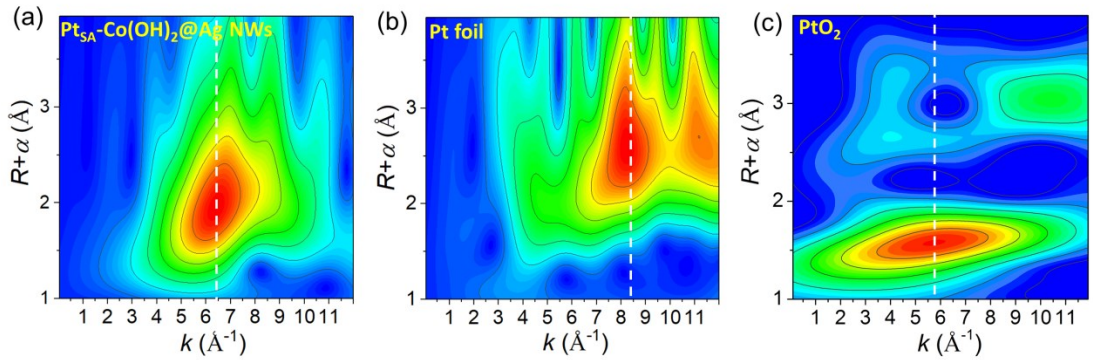

Figure S7. Wavelet transform (WT) of (a) Pt_{SA}-$Co(OH)_2$@Ag NWs, (b) Pt foil, and (c) PtO_2.

.

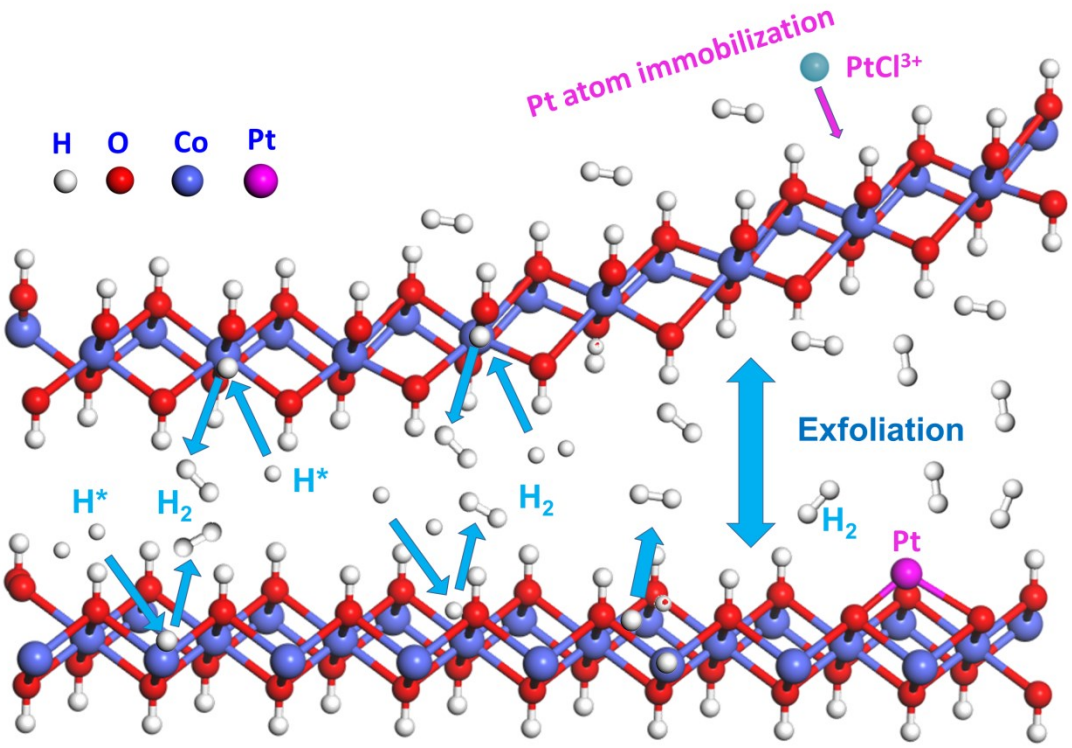

Figure S8. Illustration of the possible mechanism of single-atom Pt immobilization and electrochemical exfoliation of $Co(OH)_2$ nanosheets during HER process.

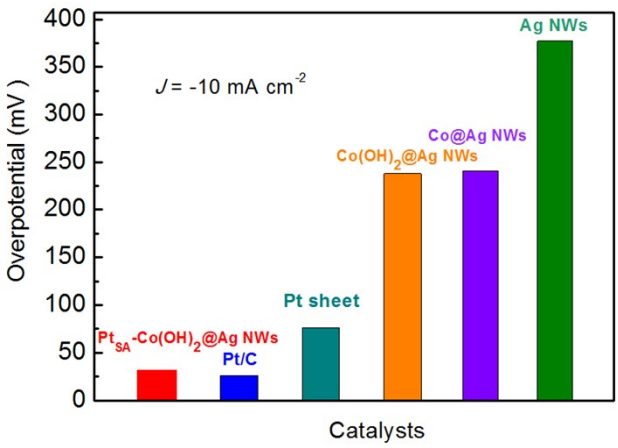

Figure S9. The overpotentials of different catalysts required to deliver a current density of J = -10 mA cm^{-2}.

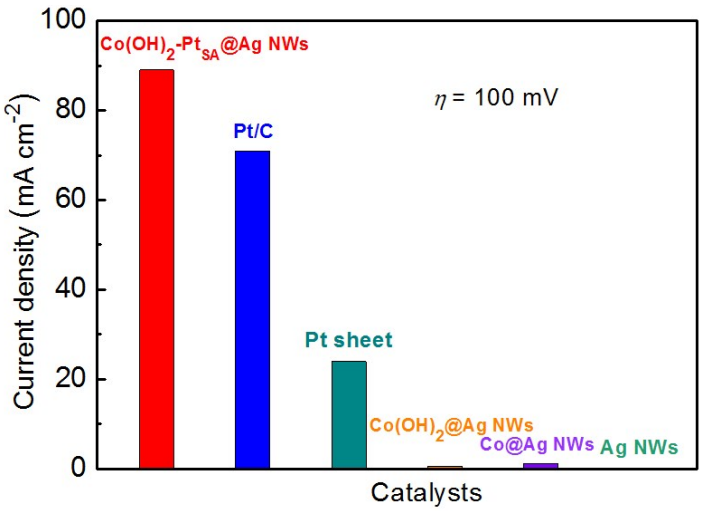

Figure S10. The corresponding current densities of different catalysts at the overpotential of η = 100 mV.

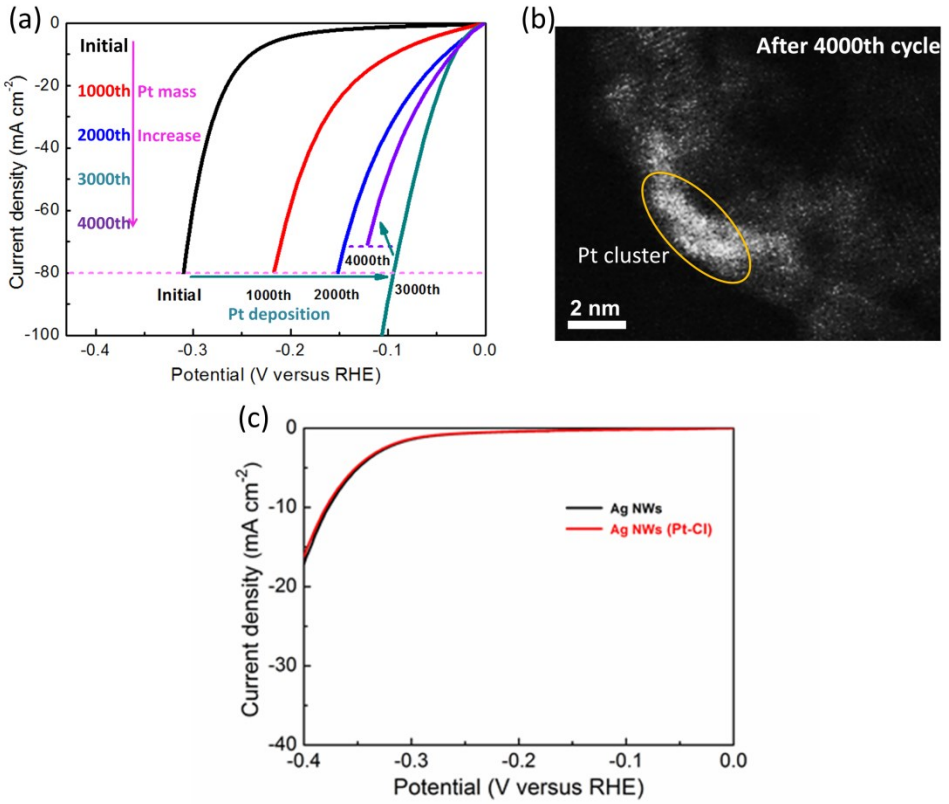

Figure S11. (a) The HER polarization curves of the sample at the different electrochemical scan cycles during the fabrication process of the single-atom Pt anchored $Co(OH)_2$. (b) Atomic-resolution HAADF-STEM image of the sample after 4000 cycles. (c) The HER polarization curves of bare Ag NWs electrode and the Ag NWs electrode containing Pt-Cl coordinations.

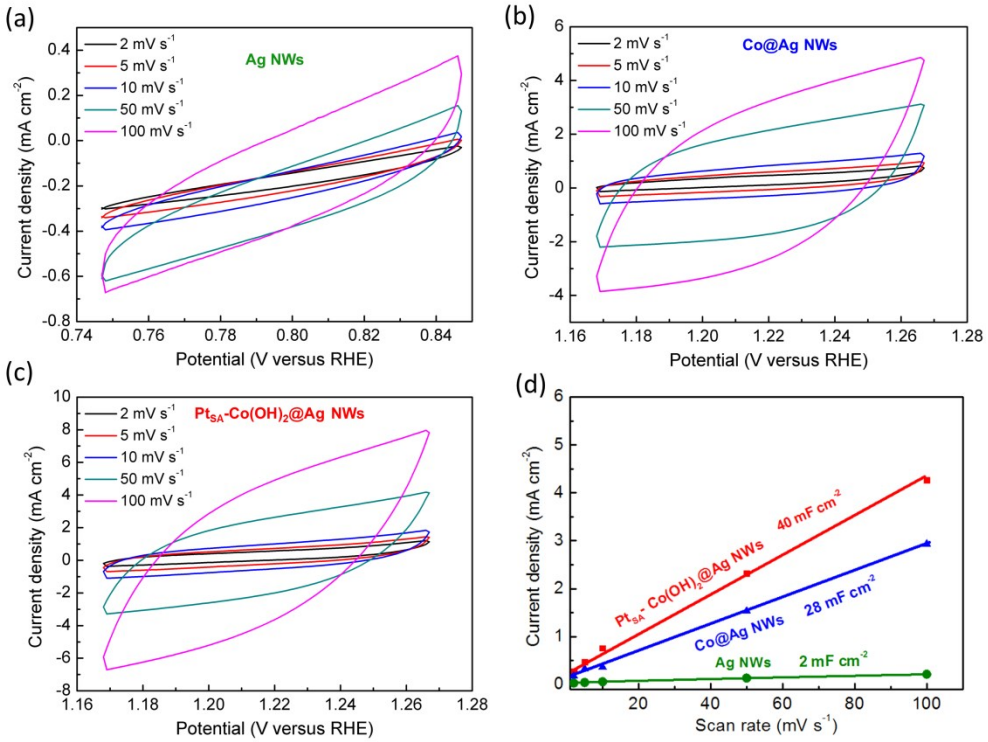

Figure S12. Cyclic voltammograms curves with different scan rates for electrochemical capacitance measurements of (a) Ag NWs, (b) Co@Ag NWs, (c) Pt_{SA}-$Co(OH)_2$@Ag NWs and (d) The double-layer capacitance (C_{dl}) of the catalysts.

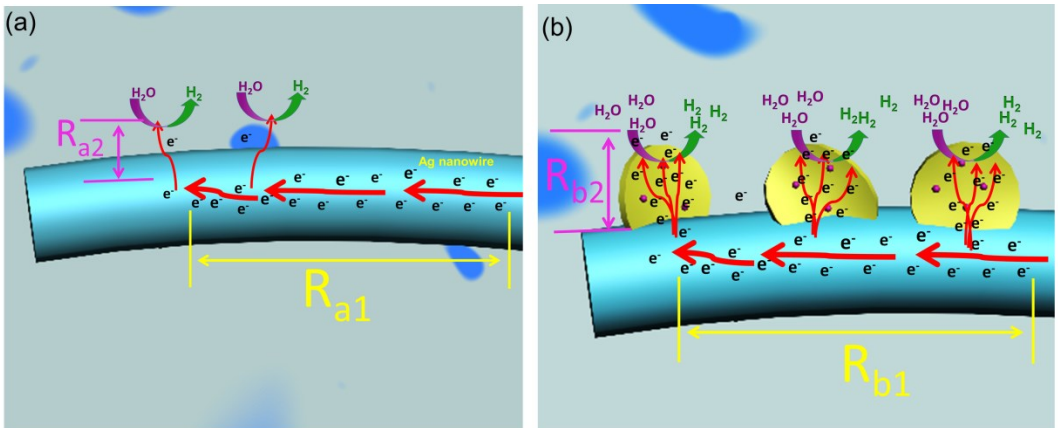

Figure S13. The illustration of electrons transport through (a) Ag NWs and (b) Pt_{SA}-$Co(OH)_2$@Ag NW during HER process.

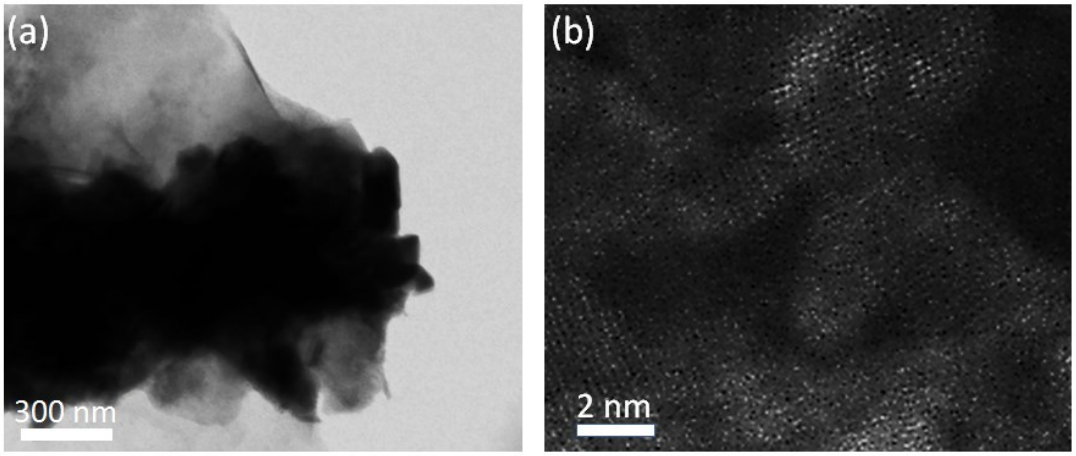

Figure S14. (a) TEM image and (b) HAADA-STEM images of Pt_{SA}-$Co(OH)_2$@Ag NWs after durability testing.

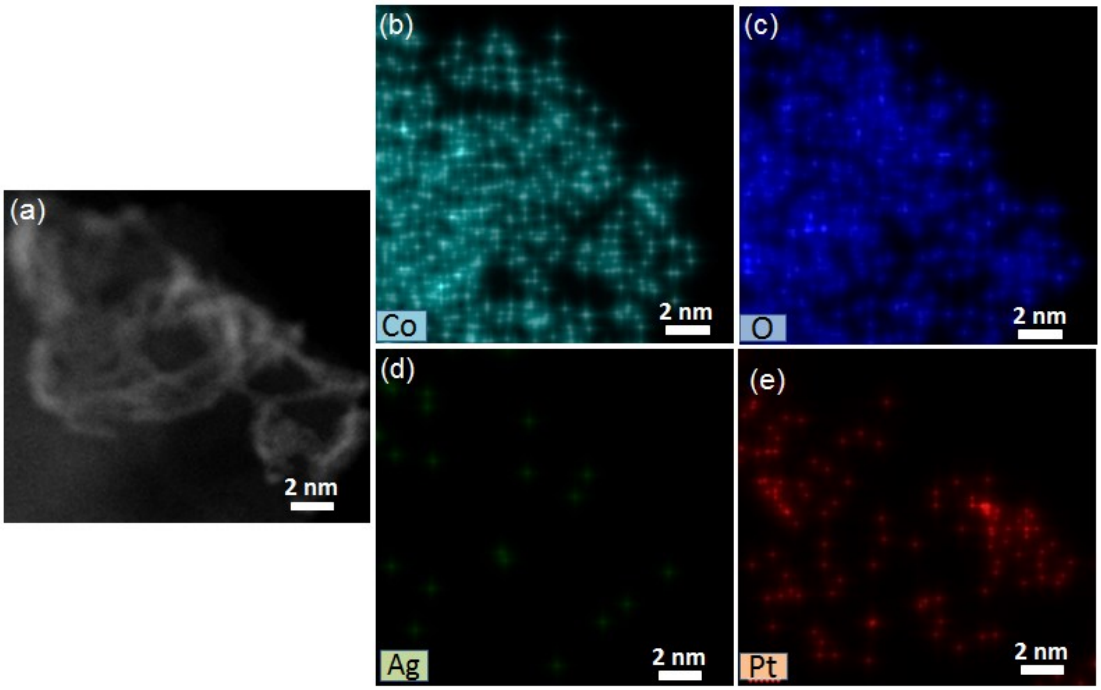

Figure S15. (a) HAADA-STEM images and (b-e) corresponding elemental mapping of Co, O, Ag, Pt of Pt_{SA}-$Co(OH)_2$@Ag NWs after durability testing.

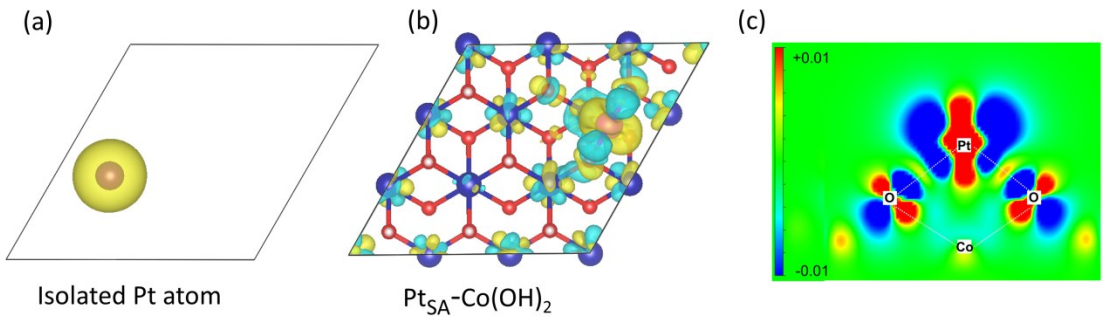

Figure S16. (a) Top view of the electronic charge density distribution of isolated Pt atom. (b) Calculated electron density difference of Pt atom in Pt_{SA}-$Co(OH)_2$. (c) Two-dimensional isosurface map on the cross-section of the Pt, O and O atoms in Pt_{SA}-$Co(OH)_2$, and the unit of electron density is e/Å^3.

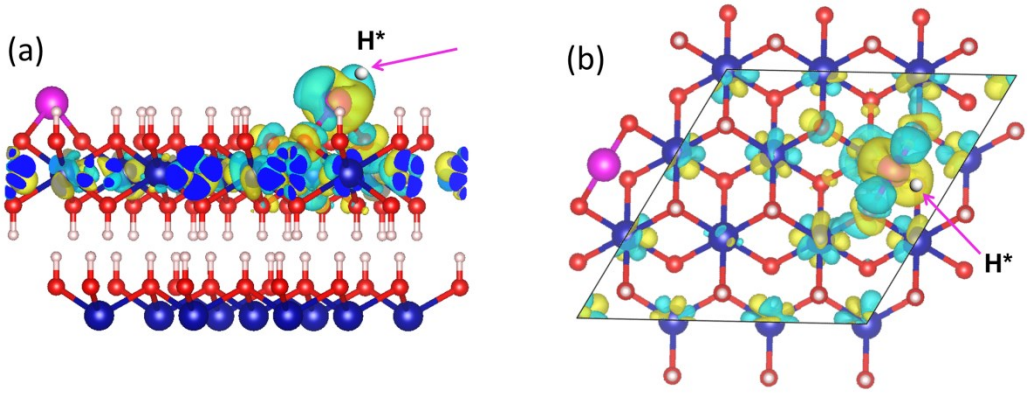

Figure S17. The charge density distribution of the Pt_{SA}-$Co(OH)_2$ and hydrogen adsorption location on the Pt atom. (a) The side view and (b) top view.

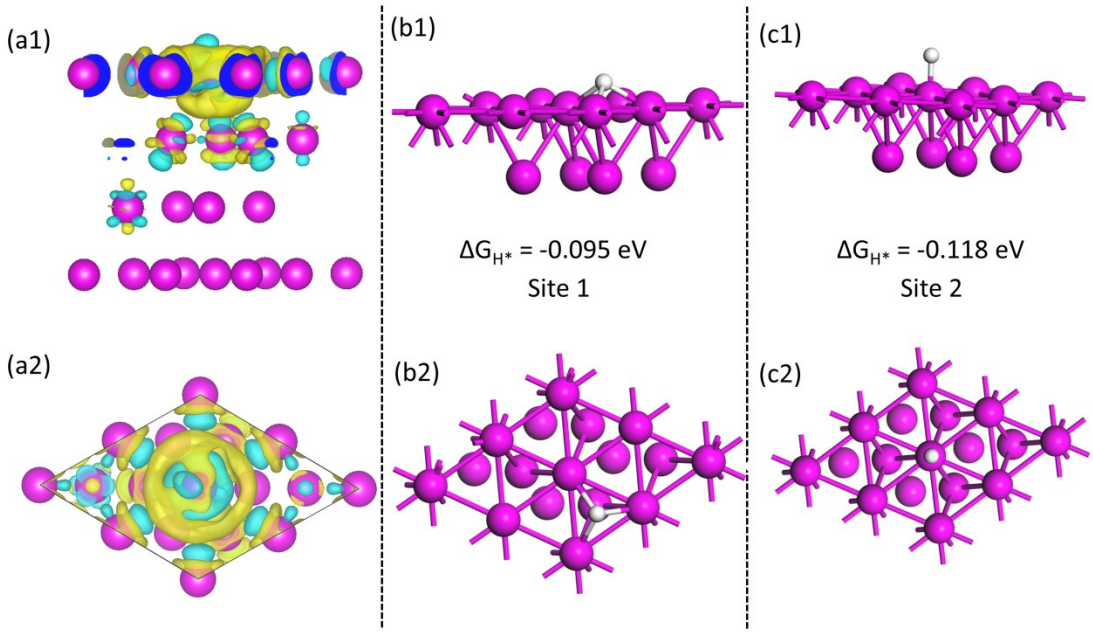

Figure S18. The calculated charge density distribution of the bulk Pt and hydrogen adsorption locations.

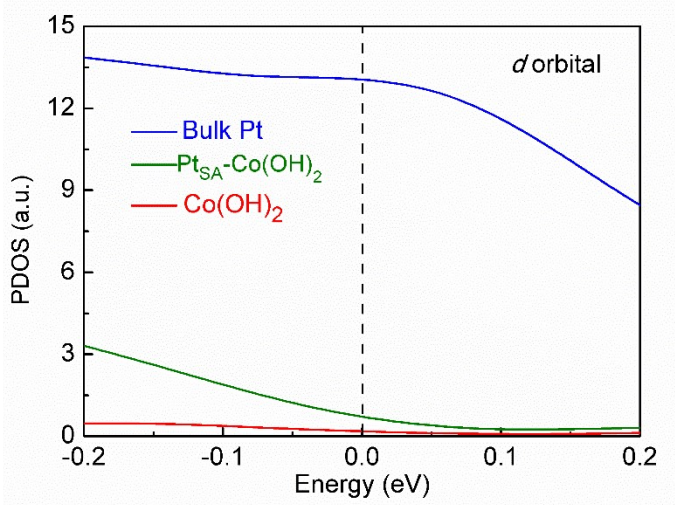

Figure S19. Calculated PDOS of $Co(OH)_2$, Pt_{SA}-$Co(OH)_2$ and bulk Pt between -0.5 eV ~ 0.5 eV.

Table S1. EXAFS fitting results of Pt_{SA}-$Co(OH)_2$@Ag NWs. Pt foil was used as a reference.

	Shell	CN	R(Å)	σ^2	ΔE_0	R factor
Pt foil	Pt-Pt	12	2.76±0.01	0.0042	8.2±0.5	0.0015
Pt_{SA}-$Co(OH)_2$@Ag NWs	Pt-O	2.1±0.4	1.95±0.04	0.0030	10.2±4.3	0.0140
	Pt-Cl1	2.5±0.3	2.32±0.02	0.0030		
	Pt-Cl2	2.9±0.5	2.74±0.02			

[a]N: coordination numbers; [b]R: bond distance; [c]σ^2: Debye-Waller factors; [d] ΔE_0: the inner potential correction. R factor: goodness of fit. S_0^2 was set to 0.78, according to the experimental EXAFS fit of Pt foil reference by fixing CN as the known crystallographic value.

Table S2. Comparison of HER performances for Pt_{SA}-$Co(OH)_2$@Ag NWs with other reported single-atom metal HER catalysts.

	Electrocatalysts	Electrolyte	Electrode binder	Overpotential at 10 mA cm^{-2} (mV)	Tafel slop (mV dec^{-1})	Charge transfer resistance (R_{ct}, Ω)	Reference
1	Pt_{SA}-$Co(OH)_2$@Ag NWs	1 M KOH	Self-supporting	29	35.7	0.7	This work
2	$Mo_2TiC_2T_x$-Pt_{SA}	0.5 M H_2SO_4	Nafion	30	30	8.5	Nat. Catal., **2018**, 1, 985.
3	Pt_{SA}/OLC	0.5 M H_2SO_4	Nafion	38	36	6.88	Nat. Energy, **2019**, 4, 512.
4	Pt/MWCNTs	0.5 M H_2SO_4	Nafion	43.9	30	8	Nano Energy, **2019**, 63, 1038.
5	Pt-MoS_2	0.1 M H_2SO_4	Nafion	60	96	-	Energy Environ. Sci., **2015**, 8, 1594.
6	er-WS_2-Pt	0.5 M H_2SO_4	Nafion	40	27	25	Adv. Mater., **2017**, 1704779.
7	Pt@PCM	0.5 M H_2SO_4	Nafion	105	63.7	-	Sci. Adv., **2018**, 4, 6657.
8	Ru-MoS_2/CC	1.0 M KOH	Self-supporting	41	114	-	Appl. Catal., B, **2019**, 249, 91.
9	Pt SA/m-WO_{3-x}	0.5 M H_2SO_4	Nafion	38	45	-	Angew. Chem., Int. Ed., **2019**, 131, 16184.
10	PtSA/S-C	0.5 M H_2SO_4	Nafion	53	46.92	28	Nat. Commun., **2019**, 10, 1.
11	Ru, N-C NWs	0.1 M H_2SO_4	Nafion	47	14	20.7	Nat. Commun., **2019**, 10, 1.
12	Pd-Graphdiyne	0.5 M H_2SO_4	Self-supporting	55	47	4.55	iScience, **2019**, 11, 31.
13	PtN_x/TiO_2	0.5 M H_2SO_4	Nafion	67	34	-	Nano Energy, **2020**, 73, 104739
14	RuP_2@NPC	0.5 M H_2SO_4	Nafion	38	38	2000	Angew. Chem., Int. Ed., **2017**,

							56, 11559.